CrystEngComm

PAPER

View Article Online
View Journal

Cite this: DOI: 10.1039/c5ce02332g

Preparation of a series of aCTV-based covalent organic frameworks and substituent effects on their properties†

Jingru Zhen,[a] Sanyuan Ding,[b] Junmin Liu,[c] Zhitang Huang,[a] Wei Wang*[b] and Qiyu Zheng*[a]

Received 30th November 2015,
Accepted 4th January 2016

DOI: 10.1039/c5ce02332g

www.rsc.org/crystengcomm

A series of amino substituted cyclotrianisylene (aCTV)-based covalent organic frameworks (COFs), aCTV-COF1 to aCTV-COF4, have been synthesized. These crystalline analogues showed permanent porosity with BET surface areas from 656 m^2 g^{-1} to 1428 m^2 g^{-1}. With the introduction of methoxy groups and hydroxyl groups at the phenyl linker moieties in aCTV-COF3 and aCTV-COF4, their properties (such as color, gas adsorption, hydrolytic stability and so on) have been influenced to a great extent. The CO_2 sorption of aCTV-COF4 has increased significantly, and the H_2 uptake of aCTV-COF3 is obviously higher than those of aCTV-COF1 and aCTV-COF2. Moreover, the introduction of the methoxy and hydroxyl groups has made aCTV-COF3 and aCTV-COF4 have better hydrolytic stability.

Introduction

With CO_2 emissions and global warming, the development of new and clean materials for CO_2 storage seems to be an obvious solution.[1,2] On the other hand, hydrogen as a clean and renewable energy has continually increasing importance.[3,4] Porous crystalline materials have well defined pore structures, stable and tunable metrics and have been widely used in gas separation and storage,[5–7] heterogeneous catalysis[8,9] and optoelectronics.[10–12] Various porous crystalline materials have been used for adsorbing and separating CO_2 from natural gas as well as storing hydrogen. In general, a large BET surface area helps to improve gas adsorption[13,14] and a smaller pore size would promote the adsorption of small molecules (such as H_2).[15,16] Porous crystalline materials with high nitrogen content would greatly enhance the adsorption of CO_2 through the interactions of N atoms and CO_2 molecules.[17,18] Therefore, regulation of pore size and modification of functional groups on porous materials will improve the performance of the materials to a large extent. The development of porous materials has undergone three representative stages: inorganic materials (*e.g.* zeolites), inorganic–organic hybrid materials (*e.g.* MOFs) and organic materials (*e.g.* COFs).[19] MOFs are a kind of materials composed of inorganic metal ions (or clusters) and organic linkers with enormous internal surface areas and permanent porosity.[20–22] The organic linkers make MOFs easy to be functionalized and make pore sizes of MOFs easy to be adjusted.[23–25] MOFs modified with desired functional groups through a post-synthesis modification (PSM) strategy have better properties.[26,27] In 2005, COF-5 was synthesized for the first time.[28] Compared with MOFs, COFs are constructed solely from light elements (H, B, C, N, O and Si), and have much lower density and transform porous crystalline materials into lightweight materials.[19,29] Introduction of organic building blocks makes COFs functional materials which can be adjusted and optimized to serve a specific purpose. For example, a metal-incorporated COF, Pd/COF-LZU1, was synthesized and showed excellent activity in catalysing the Suzuki–Miyaura reaction.[30] Functionalised COFs have been successfully synthesized through a PSM strategy too.[31,32] Click chemistry is the commonly used reaction in this strategy. Jiang and co-workers have synthesized azide-appended N_3-COF-5 as a parent material to obtain a series of triazole-functionalised COFs.[31] Lavigne's group has developed the first modular assembly groups in pores with pore diameters ranging from 1 to 2 nm.[16] In these materials, the organic compound thus represents a supporting part of the porous

[a] *Beijing National Laboratory for Molecular Science, CAS Key Laboratory of Molecular Recognition and Function, Institute of Chemistry, Chinese Academy of Sciences, Beijing, 100190, China. E-mail: zhengqy@iccas.ac.cn; Fax: +86 010 62554449; Tel: +86 010 62652811*

[b] *State Key Laboratory of Applied Organic Chemistry, College of Chemistry and Chemical Engineering, Lanzhou University, Lanzhou, Gansu, 730000, China. E-mail: wang_wei@lzu.edu.cn*

[c] *KLGHEI of Environment and Energy Chemistry, School of Chemistry and Chemical Engineering, Sun Yat-Sen University, Guangzhou, 510275, China. E-mail: liujunm@mail.sysu.edu.cn*

† Electronic supplementary information (ESI) available: Experimental details, FTIR spectra, ^{13}C CP-MAS NMR spectra, thermogravimetric analysis, scanning electron microscopy images, PXRD spectra, BET plot and pore size distribution, and model of CTV-COFs. See DOI: 10.1039/c5ce02332g

framework, therefore maintaining the pore structure and surface area.

Cyclotriveratrylene (CTV) is a C_3 symmetric rigid pyramidal macrocyclic molecule with a bowl-shaped shallow cavity.[33–35] The unique concave structure makes CTV a suitable tritopic 90° corner unit to assemble into a dynamic cube.[36] Our group reported the first CTV-based COF with hexahydroxyl cyclotricatechylene (CTC) and 1,4-phenylenebisboronic acid as building blocks.[37] The bowl-shaped core unit led to a better hydrogen uptake capacity than its planar analogue, COF-5.[28] However, boron esters are not stable and CTC-COF is perishable when exposed to air.[38] Soon afterwards, we reported two imine-linked COFs, CTV-COF-1 and CTV-COF-2, which were synthesized from triformylcyclotrianisylene (f-CTV) and aromatic amines.[39] Banerjee's group has explored two new chemically stable COFs, TpPa-1 and TpPa-2, by a combination of reversible (Schiff base reaction) and irreversible (enol-to-keto tautomerization) reactions.[40] These COFs are not so sensitive to aqueous environment and have better hydrolytic stability. Warmuth *et al.* used f-CTV and *p*-phenylenediamine to get a chiral nanocube[36] while we obtained COFs, which indicate that reaction conditions will affect the crystallinity of resulting products to a large extent. f-CTV has poor solubility, complicated synthetic steps, complex post treatment and a low overall yield (3%),[41] which makes COFs unable to be synthesized in a large scale. aCTV has better solubility, simpler synthetic steps and higher yields,[42,43] and it has not been used to build COFs. Here, we report the preparation of a series of aCTV-based COFs and their different gas adsorption properties and hydrolytic stability.

Results and discussion

Synthesis

The aCTV-COFs were synthesized by the condensation of aCTV and aromatic aldehydes under solvothermal conditions for 5 days (Scheme 1). The resulting precipitate was immersed in anhydrous tetrahydrofuran for 3 days and dried at 100 °C under vacuum for 12 h. The powders are insoluble in most organic solvents. aCTV-COF1 to aCTV-COF4 were isolated in yields of 78% to 90%.

Sample characterization

Formation of imine linkages was verified by FTIR spectroscopy and solid state magic angle spinning (MAS) ^{13}C NMR spectroscopy (see the ESI,† Fig. S1 to Fig. S7). The FTIR spectra obtained for aCTV-COF1 to aCTV-COF4 show vibrational bands for imine at 1620 and 1200 cm^{-1}, 1622 and 1207 cm^{-1}, 1615 and 1213 cm^{-1} and 1614 and 1210 cm^{-1}, respectively. Carbonyl stretching bands at 1698 cm^{-1}, 1698 cm^{-1}, 1681 cm^{-1} and 1660 cm^{-1} and N–H stretching bands at about 3100–3500 cm^{-1} for aCTV-COF1 to aCTV-COF4 were observed, which indicated that there are some unreacted amino residues at the end of the COFs. aCTV-COF3 shows a big broad peak at about 3100–3500 cm^{-1}, which is due to the overlap of the hydroxyl groups and the amino residues (see the ESI,† Fig. S1). The solid-state ^{13}C

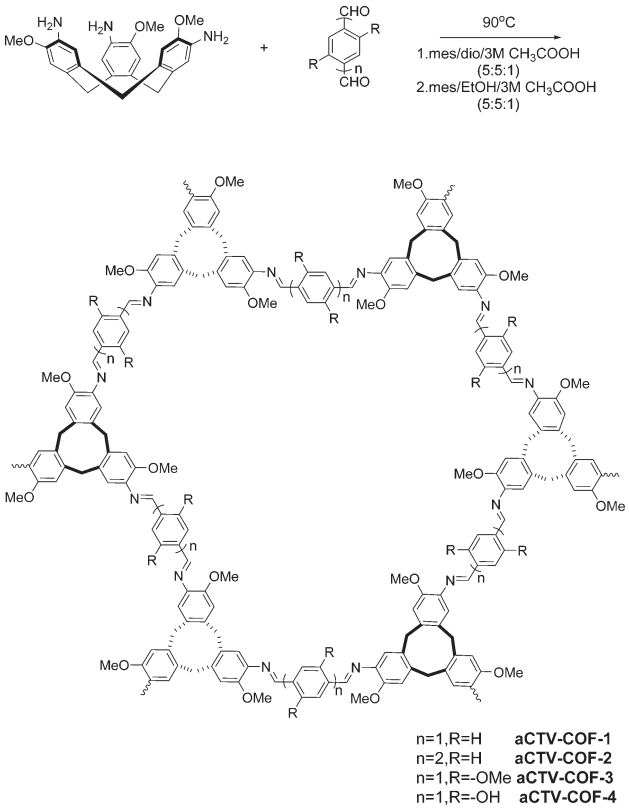

Scheme 1 Synthesis of aCTV-COF1 to aCTV-COF4.

CP-MAS NMR spectra further confirm the formation of the expected imine bonds with the signals at about 150 ppm. The two peaks at about 53 and 36 ppm correspond to carbon on the methoxy group of the benzene ring and methylene on the skeleton of CTV. The introduction of the methoxy group makes the carbon spectra of aCTV-COF3 split well (see the ESI,† Fig. S6). Scanning electron microscopy (SEM) was carried out for aCTV-COF1 to aCTV-COF4. Among them, aCTV-COF2 crystallized with an irregular ball-like morphology, which is a relatively rare type of morphology seen in COFs

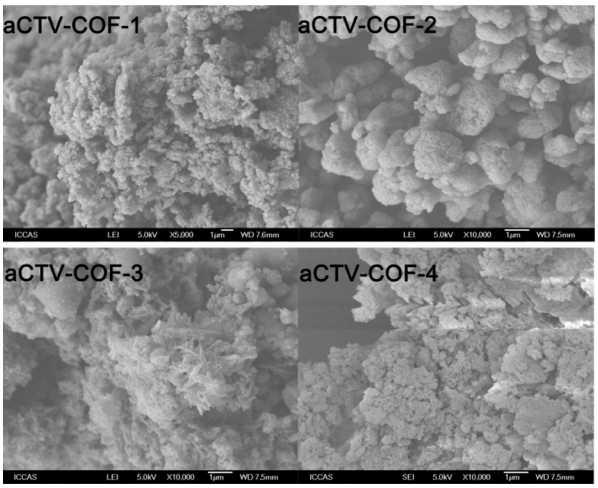

Fig. 1 SEM images of aCTV-COF1 to aCTV-COF4.

(Fig. 1). The thermal stability of the aCTV-COFs was monitored using thermogravimetric analysis (TGA) (see the ESI,† Fig. S8). The substituted COFs showed an almost identical decomposition behaviour to aCTV-COF1, indicating that the substituents are stable until the network decomposition.

Structure analysis

The powder X-ray diffraction (PXRD) patterns of aCTV-COF1 to aCTV-COF4 indicate the crystallinity of the aCTV-COFs (Fig. 2). It displays a main peak at 3.98° (100) and a second peak at 6.92° for aCTV-COF1, 3.30° and 5.67° for aCTV-COF2, 3.88°, 6.77° and 8.16° for aCTV-COF3, and 4.03°, 8.07° and 17.97° for aCTV-COF4. The PXRD patterns reveal a hexagonal structure with *P*3 symmetry and an eclipsed AA layer stacking, which is in line with most COF structures reported to date. The hexagonal unit cell parameters can be determined by the reflections as a = 26.01 Å and c = 4.58 Å for aCTV-COF1, a = 32.45 Å and c = 4.58 Å for aCTV-COF2, a = 25.08 Å and c = 4.54 Å for aCTV-COF3 and a = 26.57 Å and c = 4.49 Å for aCTV-COF4. According to the PXRD results, aCTV-COF1 and aCTV-COF2 have a better crystalline structure, while methoxy and hydroxyl substituted aCTV-COF3 and aCTV-COF4 have a slightly worse crystallinity. There are some slight differences in the main peak positions of aCTV-COF1, 3 and 4, which are supposed to be the influence of the functional groups. The flexible substituents present may rotate freely within the pores and result in amorphous units.[16] Additionally, the substituted COFs exhibited diffraction patterns similar to that of the parent material aCTV-COF1, which implies that the structures of the substituted COFs are similar to the structure assigned to aCTV-COF1. It is predicted that the substituent groups point towards the centre of the pores, thereby modifying the pore size and changing the properties of the materials. The experimental PXRD patterns match well with the simulated patterns of the eclipsed stacking models of aCTV-COF1 to aCTV-COF4 (Fig. 3). We propose that the structures of the aCTV-COFs are stacked in an eclipsed arrangement, forming 1D pores along the c axis, which is consistent with our previous results.[37,39] The aCTV units are stacked in a columnar manner with the same

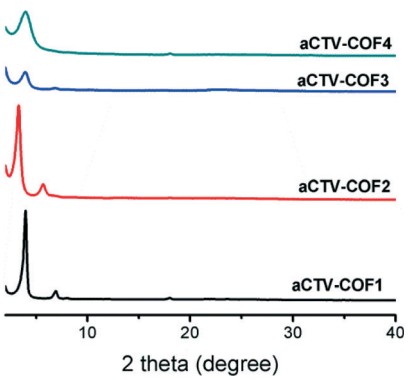

Fig. 2 PXRD patterns of aCTV-COF1 to aCTV-COF4.

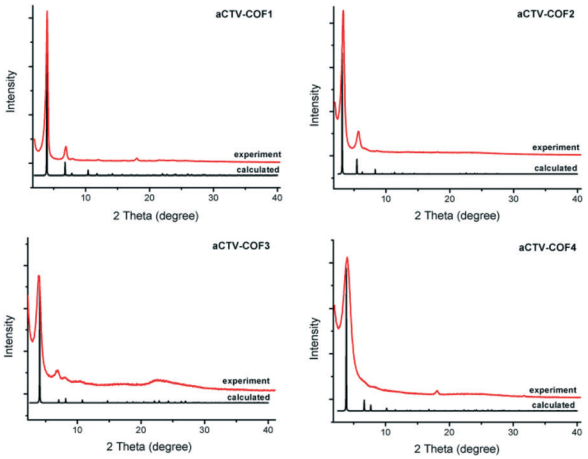

Fig. 3 Comparison of the experimentally observed PXRD patterns (red) with the simulated eclipsed patterns (black) of the aCTV-COFs.

chirality, while the adjacent CTV skeletons have the opposite chirality (see the ESI,† Fig. S11 to S18). The interlayer distance of the aCTV-COFs is about 3.5 Å, suggesting a typical van der Waals interaction between the aromatic layers. Viewed from the side, a single layer of aCTV-COFs showed an undulated structure which is stacked in an eclipsed manner.

Gas adsorption properties

The architectural stability and porosity of the aCTV-COFs were confirmed by measuring N_2 gas adsorption at 77 K. aCTV-COF1, aCTV-COF3 and aCTV-COF4 exhibited type I isotherms, which showed that microporous materials were formed.[24] On the other hand, aCTV-COF2 showed type IV isotherms, indicating the formation of mesoporous networks (Fig. 4). Estimation of the pore size of the aCTV-COFs from a density functional theory (DFT) model shows that aCTV-COF3 and aCTV-COF4 have narrower pore widths than aCTV-COF1. The difference may be caused by the substituents. The substituents would fill the pores, thereby reducing the size and surface area of the frameworks. The gas adsorption data is shown in Table 1. The BET surface area of aCTV-COF1 was

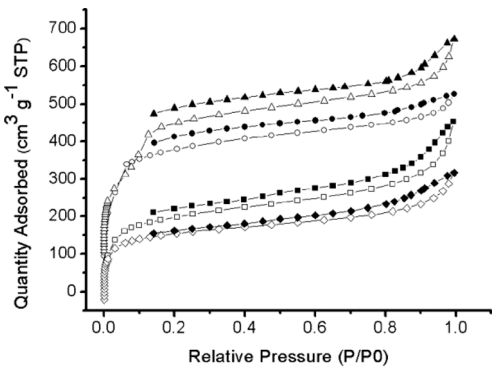

Fig. 4 Nitrogen sorption isotherms of aCTV-COF1 to aCTV-COF4 measured at 77 K (circles for aCTV-COF1, triangles for aCTV-COF2, squares for aCTV-COF3 and diamonds for aCTV-COF4).

Table 1 Gas adsorption data of aCTV-COF1 to aCTV-COF4

COF	S_{BET} $m^2\ g^{-1}$	Pore size Å	N_2 uptake $cm^3\ g^{-1}$	H_2 uptake wt%	CO_2 uptake $cm^3\ g^{-1}$
1	1132	17	525	0.5%	36
2	1428	22	672	0.8%	30
3	698	14	453	1.1%	29
4	636	14	317	1.0%	57

higher than its analogues, aCTV-COF3 and aCTV-COF4. It may be caused by the following two reasons: one is that the substituents would fill the pore and block the nitrogen getting into the pores from the corner; the other reason is that the substituents would affect the crystallinity of the materials. The measured pore sizes are shown in Table 1. The estimated total pore volumes and the pore sizes from the density functional theory (DFT) model are close to the experimental values (see the ESI,† Fig. S10). It can be seen from Table 1 that aCTV-COF2 with a greater BET surface area and pore size has higher N_2 adsorption ability than the other three COFs. We then analysed the gas adsorption properties with hydrogen. Measurements were taken at 77 K and P_0 = 760 mmHg. The hydrogen gas adsorption isotherms (Fig. 5) show very different trends for hydrogen compared to nitrogen under the same conditions. aCTV-COF3 showed the highest uptake of hydrogen of 1.1 wt%, while aCTV-COF1 showed an uptake of hydrogen of 0.8 wt%. The nitrogen uptake of aCTV-COF3 and aCTV-COF4 was much lower than that of aCTV-COF1, while hydrogen uptakes were higher for aCTV-COF3 and aCTV-COF4. The nitrogen adsorption isotherms show a trend that is similar to the calculated surface area, and they decrease with the incorporation of substituents. However, the uptakes of hydrogen were increased with the incorporation of substituents. This may result from two reasons: one is that smaller gas molecules may go through the corner cavities more easily; the other is that there are interactions between hydrogen and the incorporated methoxy and hydroxyl groups. Carbon dioxide uptake was tested at 273 K and 1 bar (Fig. 6). Different from the hydrogen uptake, aCTV-COF1, aCTV-COF2 and aCTV-COF3 showed almost the same amount of CO_2 adsorption (29.8

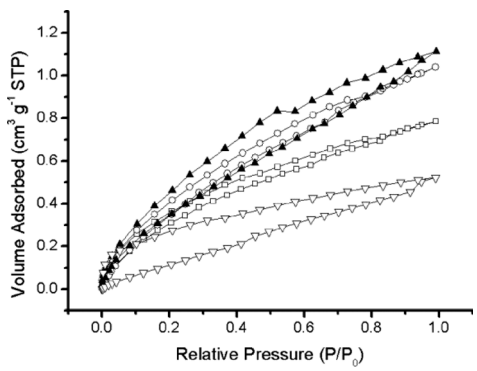

Fig. 5 H_2 uptakes of aCTV-COF1 to aCTV-COF4 measured at 1 bar (triangles for aCTV-COF1, squares for aCTV-COF2, solid triangles for aCTV-COF3 and circles for aCTV-COF4).

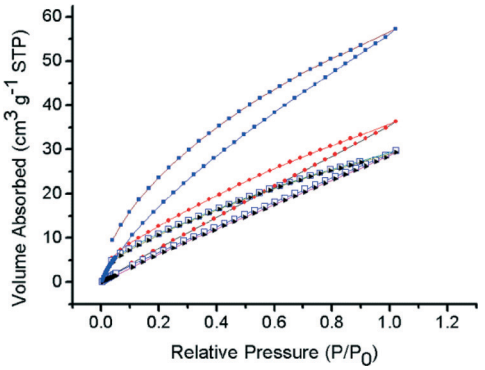

Fig. 6 Carbon dioxide sorption isotherms of aCTV-COF1 to aCTV-COF4 measured at 1 bar (red circles for aCTV-COF1, black triangles for aCTV-COF2, open squares for aCTV-COF3 and blue diamonds for aCTV-COF4).

$cm^3\ g^{-1}$), while aCTV-COF4 demonstrated nearly twice that amount (up to 57.2 $cm^3\ g^{-1}$). This is due to the interaction between the incorporated hydroxyl groups and the CO_2 molecules.

Hydrolytic stability

The hydrolytic stability of the aCTV-COFs was investigated by soaking the aCTV-COFs in water for 10 and 24 h, and no color change was observed. These materials were recovered by filtration. The remaining solids were washed with acetone to remove the possible monomers and dried at 100 °C overnight in vacuum. Powder X-ray diffraction analyses were carried out for the aCTV-COFs (Fig. 7). The peaks and the ratios of the peak intensities are all retained but with different attenuations. The attenuation in the main peak intensities after hydrolysis indicated the loss of crystallinity. The initial PXRD peak intensities of aCTV-COF3 and aCTV-COF4 are not as sharp as those of aCTV-COF1 and aCTV-COF2. After immersion in water, the peak intensities had different attenuations. aCTV-COF3 and aCTV-COF4 retained the peak intensity to a large extent while aCTV-COF1 and aCTV-COF2 was attenuated distinctly. Therefore, we conclude that the stabilities of aCTV-COF3 and aCTV-COF4 were enhanced compared to the unmodified aCTV-COF1, which is consistent with the results obtained by Banerjee's group[44] and Jiang's group.[45] The introduction of the two electron-donating methoxy groups will soften the interlayer charge repulsion by delocalizing the oxygen lone pairs,[46] while the introduction of the two hydroxyl groups adjacent to the Schiff base centres will create an intramolecular hydrogen bond, which will help to improve the chemical stability of COFs. The FTIR spectra further confirmed the retention of the structure (see the ESI,† Fig. S1 to S3).

Conclusions

In conclusion, we have synthesized a series of aCTV-COFs based on aCTV and different dialdehydes. The crown CTV motifs are stacked in a columnar manner to avoid sliding

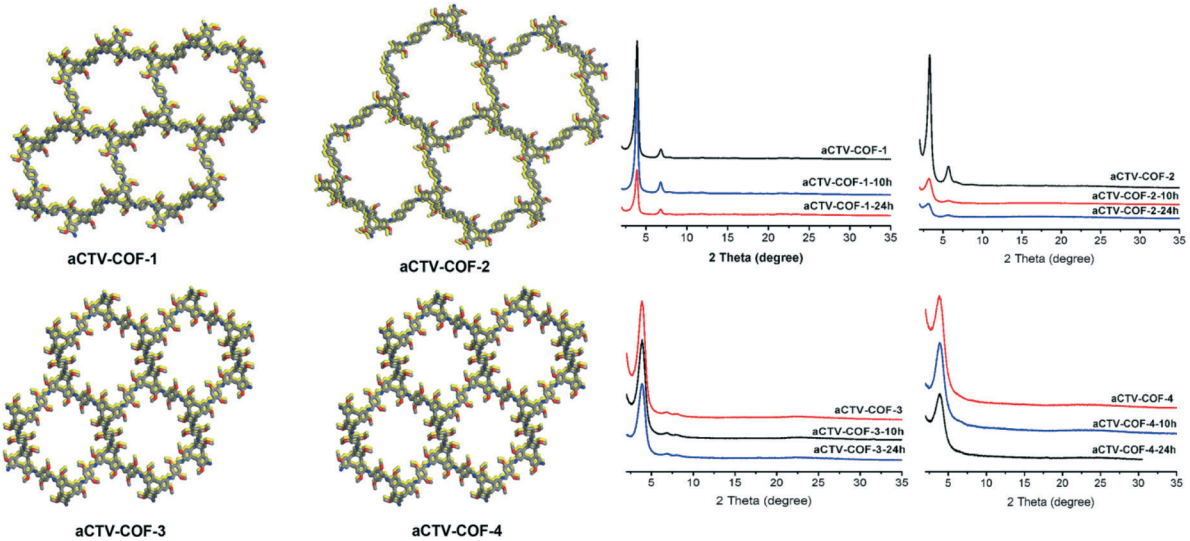

Fig. 7 Models of the aCTV-COFs and PXRD patterns of the hydrolytic test of the aCTV-COFs.

between the layers. The incorporation of methoxy and hydroxyl groups has little effect on the skeletal structure of the aCTV-COFs, but has affected the crystallinity and properties greatly. Modification of the pore interior with the methoxy and hydroxyl groups caused a reduction of nitrogen adsorption, but an increase in the adsorption of hydrogen and carbon dioxide. aCTV-COF3 and aCTV-COF4 have higher low pressure hydrogen uptake and carbon dioxide uptake than aCTV-COF1. This may be due to the interaction between the substituent groups and adsorbed gases and the impact of the smaller pore size. Moreover, aCTV-COF3 and aCTV-COF4 have better hydrolytic stability than aCTV-COF1. It offers the opportunity for post-synthesis modification of aCTV-COF4 by introducing hydroxyl groups. Further efforts are in progress to obtain more diversely functionalized materials.

Experimental

Materials and measurements

IR spectra were recorded on a Thermo-Nicolet 6700 spectrometer using KBr discs. ^{1}H NMR spectrum was recorded at ambient temperature on a BRUKER (400 MHz) NMR spectrometer. ^{13}C CP-MAS NMR spectra data were collected on a BRUKER AVANCE III 100 MHz solid state NMR spectrometer. Thermogravimetric analysis was performed on Perkin-Elmer Pyris 1 with a temperature of 750 °C. Scanning electron microscopy (SEM) was performed on a JEOL JSM6700 scanning electron microscope at 10.0 kV; the sample was prepared by drop-casting an ethanol suspension onto a mica substrate and then coated with gold. Powder X-ray diffraction (PXRD) data were recorded on a Rigaku D/max 2500 X-ray powder diffractometer, from 2 theta = 2° up to 40° with 0.02° increments. Molecular models of the aCTV-COFs were generated using the Materials Studio (ver. 6.0) suite of programs.[47] Nitrogen adsorption–desorption isotherms were measured with a Micrometrics ASAP 2020 instrument at 77 K. Hydrogen adsorption–desorption isotherms were measured at 77 K from 0 to 760 mmHg on a Micrometrics ASAP 2020 instrument. Carbon dioxide adsorption isotherms were measured at 273 K. aCTV was synthesized according to the literature.[42,43] All the chemicals were used without further purification unless stated otherwise.

Synthesis

aCTV-COF1. A 25 ml Schlenk tube was charged with aCTV (60 mg, 0.15 mmol), terephthalic aldehyde (30 mg, 0.22 mmol) and a 5 : 5 : 1 (v : v) solution of mesitylene (2.25 ml) : EtOH (2.25 ml) : 3M CH_3COOH (0.45 ml). The tube was evacuated to vacuum (−0.095 MPa) at 77 K (LN_2 bath) and then sealed. The reaction mixture was heated at 90 °C for 7 days. The product was isolated by filtration, washed with anhydrous THF, and then activated in anhydrous THF for 3 days (changed with fresh solvent every 8 h) and dried under vacuum at 100 °C. 74 mg of yellow powder was obtained with 90% yield. IR (KBr): *v* 3440, 2929, 2846, 1697, 1620, 1561, 1495, 1464, 1444, 1417, 1390, 1356, 1296, 1203, 1184, 1141, 1080, 829 cm^{-1}; ^{13}C CP-MAS NMR (100 MHz, solid state): 151.53, 145.84, 137.92, 131.15, 127.69, 119.36, 112.23, 52.90, 36.06 ppm.

aCTV-COF2. aCTV (39 mg, 0.096 mmol), biphenyl dialdehyde (30 mg, 0.14 mmol) and a 5 : 5 : 1 (v : v) solution of mesitylene (1.5 ml) : EtOH (1.5 ml) : 3 M CH_3COOH (0.3 ml) were used. The procedure is the same to that stated above. 56 mg of yellow powder was obtained with 87.5% yield. IR (KBr): *v* 3446, 2910, 2833, 1698, 1622, 1603, 1555, 1573, 1498, 1463, 1393, 1309, 1207, 1228, 1170, 1144, 1080, 817 cm^{-1}; ^{13}C CP-MAS NMR (100 MHz, solid state): 151.89, 145.90, 136.99, 132.13, 118.82, 112.13, 54.03, 36.26 ppm.

aCTV-COF3. aCTV (42 mg, 0.10 mmol), 2,5-dimethoxyterephthalaldehyde (30 mg, 0.15 mmol) and a 5 : 5 : 1 (v : v) solution of mesitylene (1.5 ml) : dioxane (1.5 ml) :

3 M CH_3COOH (0.3 ml) were used. The procedure is the same to that stated above. 52 mg of reddish brown powder was obtained with 78% yield. IR (KBr): *v* 3367, 2935, 2832, 1681, 1615, 1507, 1464, 1409, 1373, 1287, 1266, 1140, 1082, 1038, 880 cm^{-1}; ^{13}C CP-MAS NMR (100 MHz, solid state): 152.46, 145.53, 137.63, 134.39, 130.51, 127.24, 122.93, 118.75, 113.39, 111.03, 108.13, 53.11, 36.11 ppm.

aCTV-COF4. aCTV (50 mg, 0.12 mmol), 2,5-dihydroxyterephthalaldehyde (31 mg, 0.18 mmol) and a 5 : 5 : 1 (v:v) solution of mesitylene (1.5 ml) : dioxane (1.5 ml) : 3 M CH_3COOH (0.3 ml). The procedure is the same to that stated above. 61 mg of reddish brown powder was obtained with 82% yield. IR (KBr): *v* 3447, 2931, 2834, 1660, 1614, 1496, 1396, 1337, 1268, 1200, 1148, 1083, 1014, 865 cm^{-1}; ^{13}C CP-MAS NMR (100 MHz, solid state): 152.66, 138.78, 130.84, 121.94, 117.25, 111.90, 53.02, 35.94 ppm.

Gas adsorption analysis

Before measurement, samples of the as-synthesized aCTV-COFs were soaked in 10 ml of distilled anhydrous THF, which was changed with fresh solvent every 8 h. This exchange procedure was repeated several times, finally the solvent was decanted and the solid was washed with anhydrous THF (3 × 5 ml), filtered, and evacuated overnight under vacuum at 100 °C.

Acknowledgements

This work was supported by the Major State Basic Research Development Program of China (2011CB932501 and 2013CB834504).

Notes and references

1 N. MacDowell, N. Florin, A. Buchard, J. Hallett, A. Galindo, G. Jackson, C. S. Adjiman, C. K. Williams, N. Shah and P. Fennell, *Phys. Chem. Chem. Phys.*, 2010, **12**, 1.
2 L. Zhang, K. Cai, F. Zhang and Q. Yue, *Chem. Res. Chin. Univ.*, 2015, **31**, 130.
3 G. Marbán and T. Valdés-Solís, *Int. J. Hydrogen Energy*, 2007, **32**, 1625.
4 L. Schlapbach and A. Zuttel, *Nature*, 2001, **414**, 353.
5 R. Matsuda, R. Kitaura, S. Kitagawa, Y. Kubota, R. V. Belosludov, T. C. Kobayashi, H. Sakamoto, T. Chiba, M. Takata, Y. Kawazoe and Y. Mita, *Nature*, 2005, **436**, 238.
6 T. A. Makal, J. R. Li, W. Lu and H. C. Zhou, *Chem. Soc. Rev.*, 2012, **41**, 7761.
7 J. Duan, W. Jin and R. Krishna, *Inorg. Chem.*, 2015, **54**, 4279.
8 S. Hasegawa, S. Horike, R. Matsuda, S. Furukawa, K. Mochizuki, Y. Kinoshita and S. Kitagawa, *J. Am. Chem. Soc.*, 2007, **129**, 2607.
9 R. Palkovits, M. Antonietti, P. Kuhn, A. Thomas and F. Schuth, *Angew. Chem., Int. Ed.*, 2009, **48**, 6909.
10 X. Ding, X. Feng, A. Saeki, S. Seki, A. Nagai and D. Jiang, *Chem. Commun.*, 2012, **48**, 8952.
11 X. Ding, J. Guo, X. Feng, Y. Honsho, J. Guo, S. Seki, P. Maitarad, A. Saeki, S. Nagase and D. Jiang, *Angew. Chem., Int. Ed.*, 2011, **50**, 1289.
12 Y. Xu, S. Jin, H. Xu, A. Nagai and D. Jiang, *Chem. Soc. Rev.*, 2013, **42**, 8012.
13 A. P. Cote, H. M. El-Kaderi, H. Furukawa, J. R. Hunt and O. M. Yaghi, *J. Am. Chem. Soc.*, 2007, **129**, 12914.
14 H. M. El-Kaderi, J. R. Hunt, J. L. Mendoza-Cortes, A. P. Cote, R. E. Taylor, M. O'Keeffe and O. M. Yaghi, *Science*, 2007, **316**, 268.
15 R. Dawson, A. I. Cooper and D. J. Adams, *Prog. Polym. Sci.*, 2012, **37**, 530.
16 R. W. Tilford, S. J. Mugavero, 3rd, P. J. Pellechia and J. J. Lavigne, *Adv. Mater.*, 2008, **20**, 2741.
17 M. G. Rabbani, A. K. Sekizkardes, O. M. El-Kadri, B. R. Kaafarani and H. M. El-Kaderi, *J. Mater. Chem.*, 2012, **22**, 25409.
18 X. L. Hu, Q. H. Gong, R. L. Zhong, X. L. Wang, C. Qin, H. Wang, J. Li, K. Z. Shao and Z. M. Su, *Chem. – Eur. J.*, 2015, **21**, 7238.
19 S. Y. Ding and W. Wang, *Chem. Soc. Rev.*, 2013, **42**, 548.
20 J. R. Long and O. M. Yaghi, *Chem. Soc. Rev.*, 2009, **38**, 1213.
21 M. O'Keeffe, *Chem. Soc. Rev.*, 2009, **38**, 1215.
22 D. J. Tranchemontagne, J. L. Mendoza-Cortes, M. O'Keeffe and O. M. Yaghi, *Chem. Soc. Rev.*, 2009, **38**, 1257.
23 P. Deria, J. E. Mondloch, O. Karagiaridi, W. Bury, J. T. Hupp and O. K. Farha, *Chem. Soc. Rev.*, 2014, **43**, 5896.
24 S. M. Cohen, *Chem. Rev.*, 2012, **112**, 970.
25 K. K. Tanabe and S. M. Cohen, *Chem. Soc. Rev.*, 2011, **40**, 498.
26 Z. Q. Wang and S. M. Cohen, *J. Am. Chem. Soc.*, 2007, **129**, 12368.
27 Y. Goto, H. Sato, S. Shinkai and K. Sada, *J. Am. Chem. Soc.*, 2008, **130**, 14354.
28 A. P. Cote, A. I. Benin, N. W. Ockwig, M. O'Keeffe, A. J. Matzger and O. M. Yaghi, *Science*, 2005, **310**, 1166.
29 X. Feng, X. Ding and D. Jiang, *Chem. Soc. Rev.*, 2012, **41**, 6010.
30 S. Y. Ding, J. Gao, Q. Wang, Y. Zhang, W. G. Song, C. Y. Su and W. Wang, *J. Am. Chem. Soc.*, 2011, **133**, 19816.
31 A. Nagai, Z. Guo, X. Feng, S. Jin, X. Chen, X. Ding and D. Jiang, *Nat. Commun.*, 2011, **2**, 536.
32 D. N. Bunck and W. R. Dichtel, *Chem. Commun.*, 2013, **49**, 2457.
33 M. J. Hardie, R. Ahmad and C. J. Sumby, *New J. Chem.*, 2005, **29**, 1231.
34 M. J. Hardie, *Chem. Soc. Rev.*, 2010, **39**, 516.
35 A. Collet, *Tetrahedron*, 1987, **43**, 5725.
36 D. Xu and R. Warmuth, *J. Am. Chem. Soc.*, 2008, **130**, 7520.
37 J. T. Yu, Z. Chen, J. L. Sun, Z. T. Huang and Q. Y. Zheng, *J. Mater. Chem.*, 2012, **22**, 5369.
38 L. M. Lanni, R. W. Tilford, M. Bharathy and J. J. Lavigne, *J. Am. Chem. Soc.*, 2011, **133**, 13975.
39 J. R. Song, J. L. Sun, J. M. Liu, Z. T. Huang and Q. Y. Zheng, *Chem. Commun.*, 2014, **50**, 788.
40 S. Kandambeth, A. Mallick, B. Lukose, M. V. Mane, T. Heine and R. Banerjee, *J. Am. Chem. Soc.*, 2012, **134**, 19524.

41 D. J. Cram, M. E. Tanner, S. J. Keipert and C. B. Knobler, *J. Am. Chem. Soc.*, 1991, **113**, 8909.
42 J. Garcia, E. Martin, D. Morales, H. Torrens and F. Delrio, *Inorg. Chim. Acta*, 1993, **207**, 93.
43 C. Garcia, J. Maltheta and A. Collet, *Bull. Soc. Chim. Fr.*, 1993, **130**, 93.
44 S. Kandambeth, D. B. Shinde, M. K. Panda, B. Lukose, T. Heine and R. Banerjee, *Angew. Chem., Int. Ed.*, 2013, **52**, 13052.
45 X. Chen, M. Addicoat, E. Jin, L. Zhai, H. Xu, N. Huang, Z. Guo, L. Liu, S. Irle and D. L. Jiang, *J. Am. Chem. Soc.*, 2015, **137**, 3241.
46 H. Xu, J. Gao and D. L. Jiang, *Nat. Chem.*, 2015, **7**, 905.
47 Accelrys, Inc., *Materials Studio 4.3 V*, San Diego, CA, 2003.